Supplementary Information for

Independent parallel production of tunable blood clot analogues in hourglass-profiled circular PDMS fluidic channels

Chun-Hsin Hsu,‡[a] To-Wen Chen,‡[a] Wei-Jen Soong[a] and Chihchen Chen*[a,b]

[a] Institute of NanoEngineering and Microsystems, National Tsing Hua University, Hsinchu 300044 Taiwan.

[b] Department of Power Mechanical Engineering, National Tsing Hua University, Hsinchu 300044, Taiwan.

‡ These authors contributed equally to this work.

*chihchen@mx.nthu.edu.tw

Overview of blood clot fabrication generation approaches

Blood clots harvested from patients or animals remain the most physiologically relevant for thrombolysis and thrombectomy testing, though they are costly and less controllable. *In-vitro* clot analogues are typically generated using static biochemical induction, microfluidic or organ-on-chip platforms, and shear-based flow systems, as summarized in Supplementary Table S1. Static biochemical methods rely on the addition of pro-coagulant agents such as thrombin, calcium, or tissue factor to whole blood or remixed blood components, offering reproducibility and compositional control but lacking shear forces and thus failing to fully replicate patient clots. Microfluidic platforms incorporate endothelial cells, inflammatory cues, and microvascular flow, providing high physiological relevance but requiring complex setups and facing stability challenges; moreover, they often suffer from poor retrievability, limiting external mechanical testing. Shear-based flow models, which perfuse blood through stenotic or collagen-coated channels under high shear stress, offer a practical balance between reproducibility and physiological fidelity.

Supplementary Table S1 Overview of blood clot generation approaches

Blood clot generation approaches			**Key drivers**	**Physiological relevance**	**Phenotype controllability**	**Retrievability**	**Reproducibility**	**Throughput**	**Fabrication complexity**	**Thrombolysis/ thrombectomy compatibility**	**References**
Patient samples/Animal model			combined factors	+++	+	+ (invasive)	+	+	+++	+++ / +++	[12]
Static biochemical induction			thrombin, Ca^{2+}, tissue factor	+	++	+++	+++	+++	+	++ / +++	[15]
Microfluidic organ-on-a-chip			endothelial cells, flow, inflammation	++	+++	+	++	+	+++	+++ / +	[23]
Shear-based flow systems			high shear stress								
Design	**Material**	**Cross-section**	**Additional drivers**								
chaotic mixer	PDMS/glass	rectangular	tissue factor, collagen, glass	+	+	++	++	++	+++	+++ / ++	[22]
constriction	PDMS/glass	rectangular	glass	+	++	+	+++	+++	+++	++ / +	[20]
constriction	glass	circular	collagen, glass	++	++	+	++	++	+	+++ / +	[16]
constriction	PDMS/PDMS	circular	Ca^{2+}	++	+++	+++	+++	++	++	+++ / +++	(This study)

+++: high, ++: moderate, +: low

PDMS: poly(dimethyl siloxane)

Calibration of flowrate sensors

Because whole blood viscosity varies among donors and sensor mounting can introduce discrepancies, flow-rate sensors were recalibrated prior to each experiment using the same blood source to minimize bias from hematocrit and temperature variations. All sensors were calibrated against the roller pump output, recorded as the *setting flowrate*, while the corresponding sensor measurement ($Q_{detected}$) was defined as the *detected flowrate*. Linear regression analysis was performed to derive the correction function. The resulting regression coefficients, including slope (a), Y-intercept (b), and coefficient of determination (R^2), are summarized in Supplementary Table S1. The corrected flowrate (Q_{corr}) was calculated as:

$$Q_{corr} = Q_{detected} - b.$$

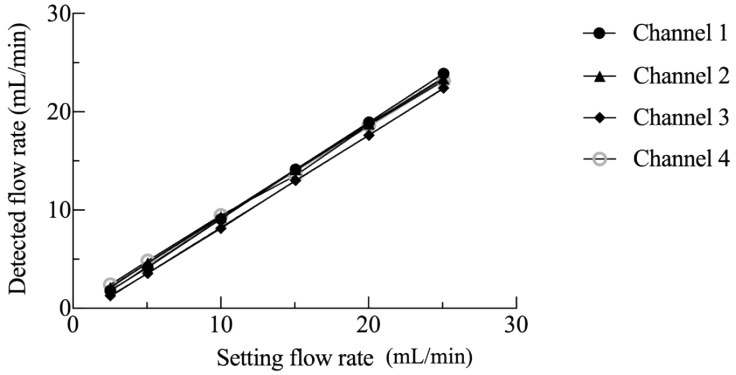

Supplementary Fig. S1 Calibration of flowrate sensors. Calibration curves of the four flowrate sensors plotted against roller pump output, *setting flowrate.* Each data point represents the detected flow rate ($Q_{detected}$) measured by the sensor at the corresponding pump setting. Linear regression analysis demonstrated excellent linearity ($R^2 > 0.999$) across the tested range of 2.5–25.0 mL/min.

Supplementary Table S2 Regression coefficients of flowrate sensors. Summary of linear regression parameters for the four flowrate sensors, including slope (a), Y-intercept (b), and coefficient of determination (R^2). Calibration was performed over a flowrate range of 2.5-25.0 mL/min using roller pump output as the reference.

Linear regression	Flowrate sensors			
	Channel 1	Channel 2	Channel 3	Channel 4
slope (a)	0.9816	0.9441	0.9386	0.9169
Y-intercept (b)	-0.7186	-0.1793	-1.164	0.1241
R^2	1.0000	0.9999	1.0000	0.9992

A single-loop clot analogue production system

The developed system operates in a single-loop mode with one upstream and one downstream reservoir, enabling clot analogue production under nominally identical conditions and supporting consistent morphology for downstream handling and characterization. As shown in Supplementary Figs. S2A–B, four hourglass-profiled circular PDMS channels were connected in parallel. Flowrate monitoring during incubation (Supplementary Fig. S2C) revealed stable initial values across all channels, indicating balanced hydraulic resistance. As clot analogues formed at 16.5 mM $CaCl_2$, flowrates declined rapidly at around 8 minutes, consistent with substantial luminal obstruction at the constriction region. The timing and overall patterns of flow reduction were comparable among channels, reflecting similar clot formation behavior under the shared hydrostatic driving condition. Transient drops in flowrate were observed in Channels 3 and 4 (arrows in Supplementary Fig. S2C), while other channels remained unaffected. The sensor for Channel 2 failed at ~7.6 min, after which recording ceased. Images of clot analogues formed in Channels 1–4 are shown in Supplementary Figs. S2D–G, with enlarged views spanning the constriction region in Supplementary Figs. S2H–K

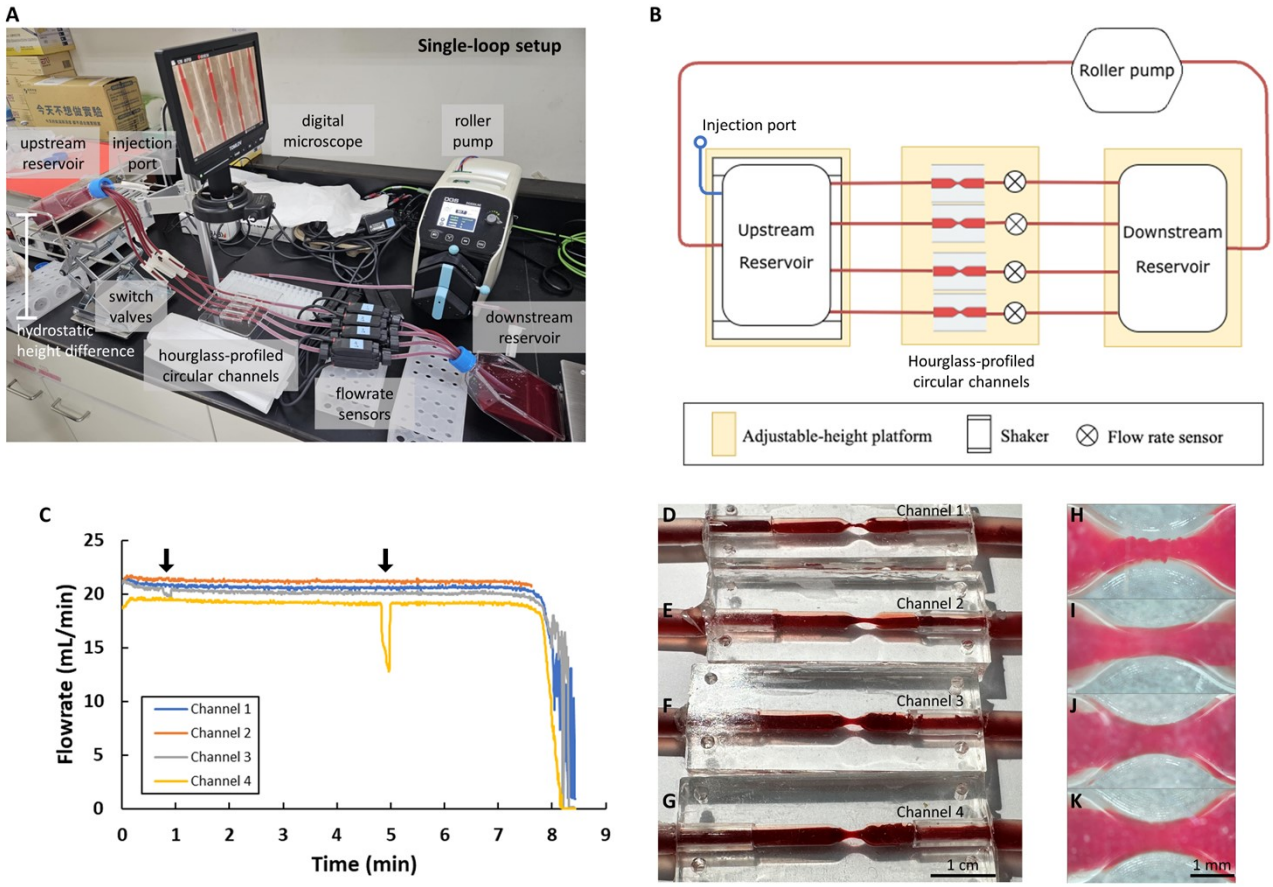

Supplementary Fig. S2 Single-loop clot analogue production system. A) Photograph of the system. A roller pump recirculates blood from the downstream to the upstream reservoir, mounted on an adjustable-height platform. The hydrostatic height difference drives flow through a tubing network incorporating switching valves, hourglass-profiled channels, and flowrate sensors. Reagents can be introduced into the loop at any time via the injection port. Real-time imaging is provided by a digital microscope. B) Schematic diagram showing four hourglass-profiled circular channels operating in parallel to generate clot analogues. C) Flowrate recordings from Channels 1-4 during clot analogue formation at 16.5 mM $CaCl_2$. Transient flowrate drops in Channels 3 and 4 are indicated by arrows, while other channels remain stable. All channels exhibit a rapid decline at 8.0 ± 0.2 min (N = 4 from the same blood batch), consistent with near-occlusive blockage. The sensor for Channel 2 encountered an error after 7.6 min and ceased recording. D-G) Images of clot analogues formed in Channels 1–4. H-K) Enlarged views of the clot analogues spanning the constriction region.

Occlusion time and real-time flowrate traces from each blood sample

The same dataset as presented in Fig. 4 is shown here, but individual flowrate traces are grouped by blood sample to highlight the minimal intrasystem variation.

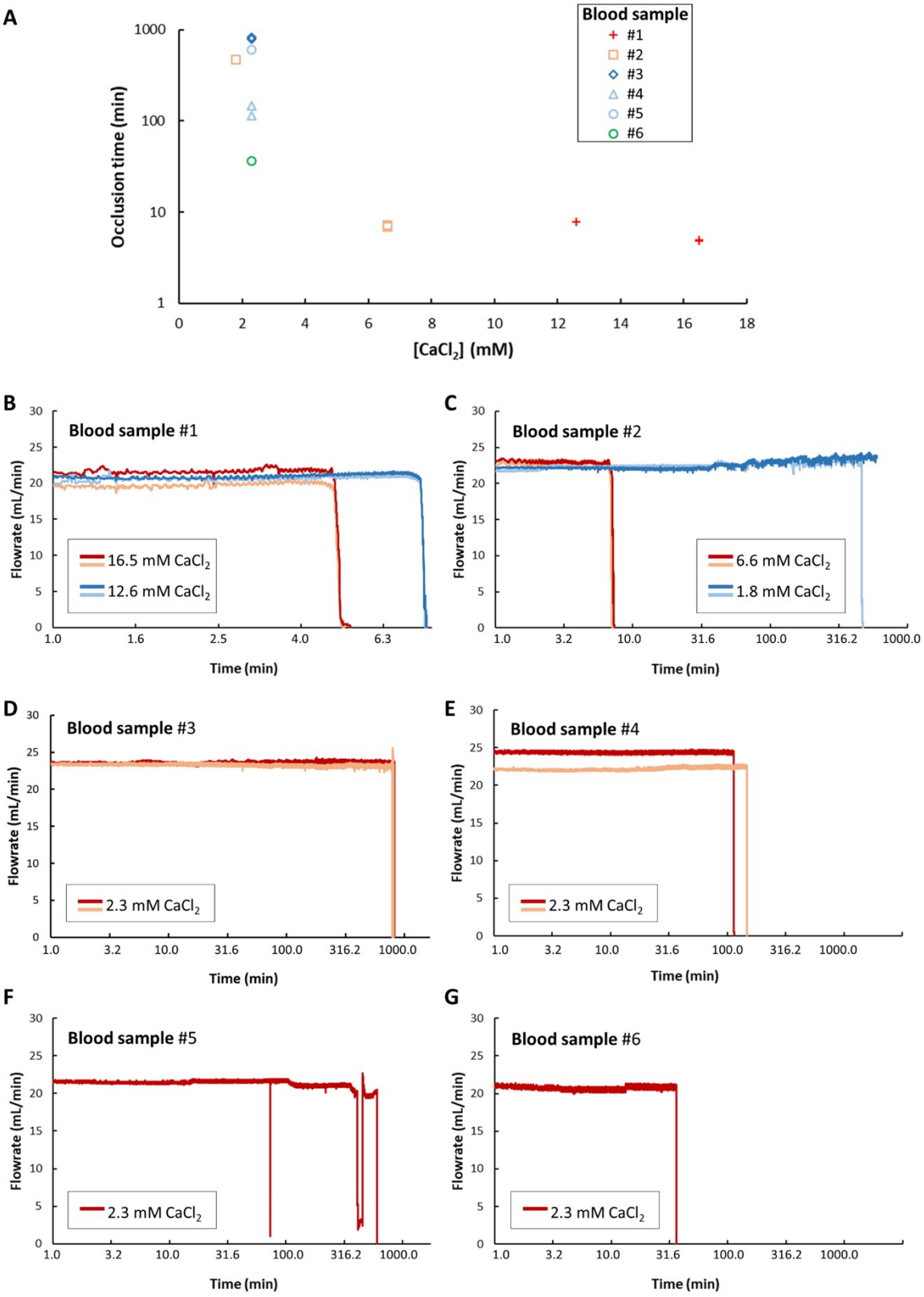

Supplementary Fig. S3 Occlusion time and real-time flowrate traces from each blood sample. A) The occlusion time decreased progressively with increasing $CaCl_2$ concentration. Note the logarithmic scale on the y-axis. B-G) Real-time flowrate traces from each blood sample. Note the logarithmic scale on the x-axis.

Simultaneous imaging and flowrate recording of clot analogue passage through the hourglass-profiled PDMS circular channel

Under low-calcium conditions (2.3 mM $CaCl_2$), time-lapse microscopy revealed progressive changes in clot morphology. After ~73.8 minutes of continuous recycled perfusion, a small clot analogue was observed passing through the constriction region (Supplementary Movie S1). With extended cycling (~410 minutes), multiple clot analogues progressively accumulated and aggregated at the constriction region (Supplementary Movie S2). These events were concurrently reflected in flow-rate measurements.

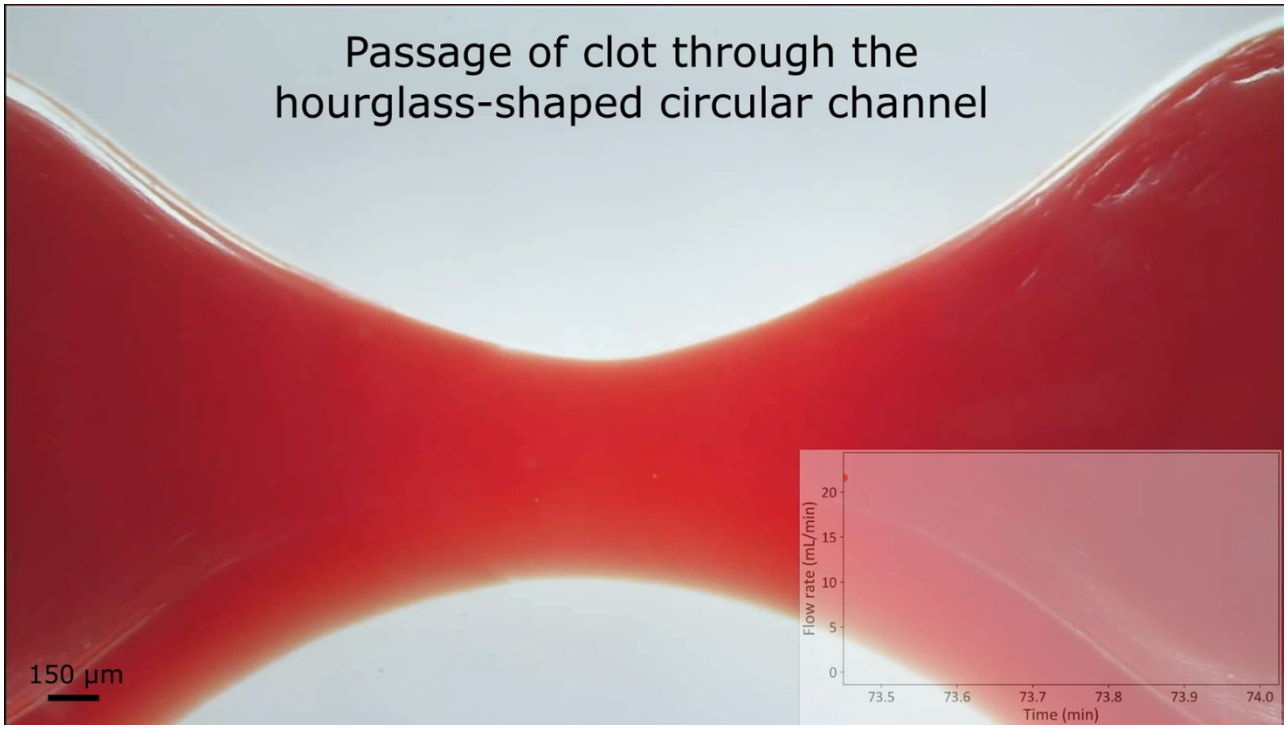

Supplementary Movie S1. Simultaneous imaging and flowrate recording of a clot analogue formed under 2.3 mM $CaCl_2$ passing through the hourglass-profiled PDMS circular channel after ~73.8 minutes of recycled perfusion.

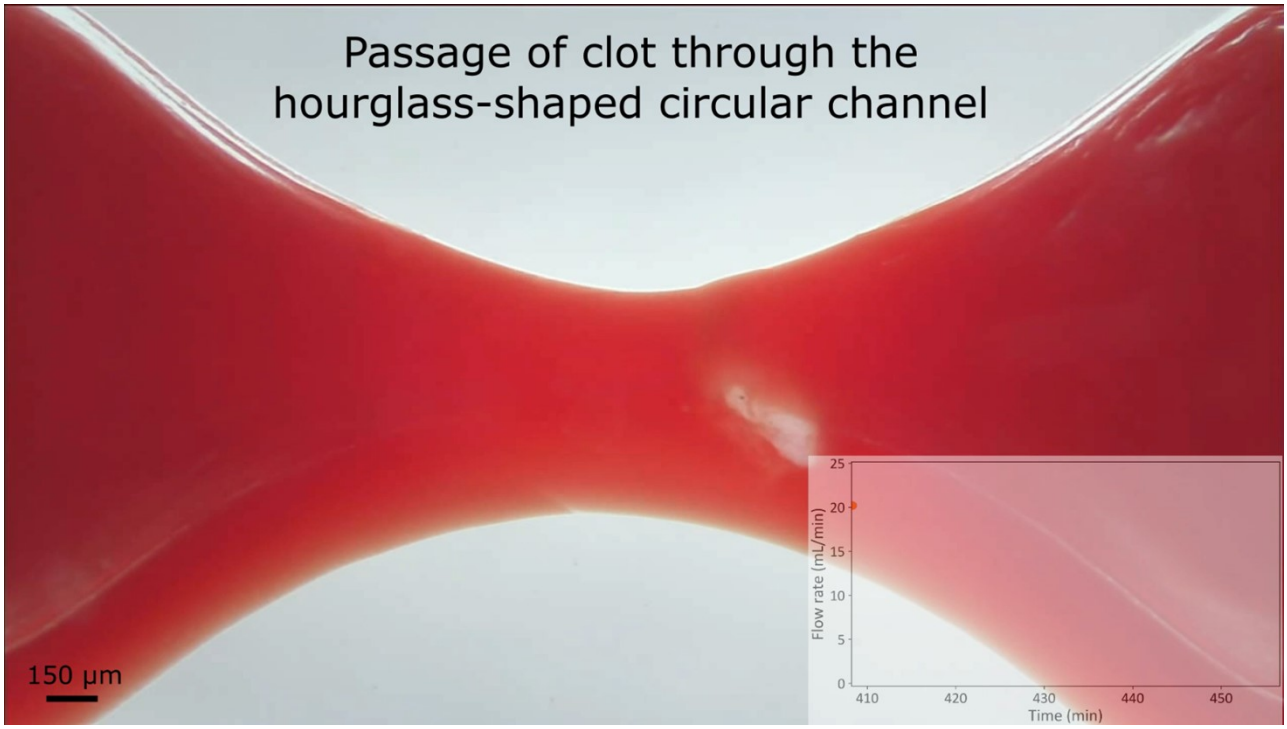

Supplementary Movie S2. Simultaneous imaging and flowrate recording (40× speed) of the same channel shown in Supplementary Movie S1. With extended cycling, multiple clot analogues progressively accumulated and aggregated at the constriction region.

Clot analogue retrieval from the hourglass-profiled circular channel

Clot analogues formed within the hourglass-profiled PDMS channels were retrieved (Supplementary Fig. S4). The detached device was first rinsed in PBS to remove residual blood components (Supplementary Fig. S4A). The PDMS slab was then carefully opened along the side with a scalpel to expose the channel lumen (Supplementary Fig. S4B), and the clot analogue was gently lifted out using forceps.

The retrieved clot analogues retained an elongated, tapered morphology consistent with the hourglass constriction geometry and could be recovered as continuous structures without visible fragmentation (Supplementary Fig. S4C). The same retrieval procedure was applied across different $CaCl_2$ concentrations. Although clots varied in color and apparent density, intact recovery as continuous structures was consistently achieved (Supplementary Fig. S4D).).

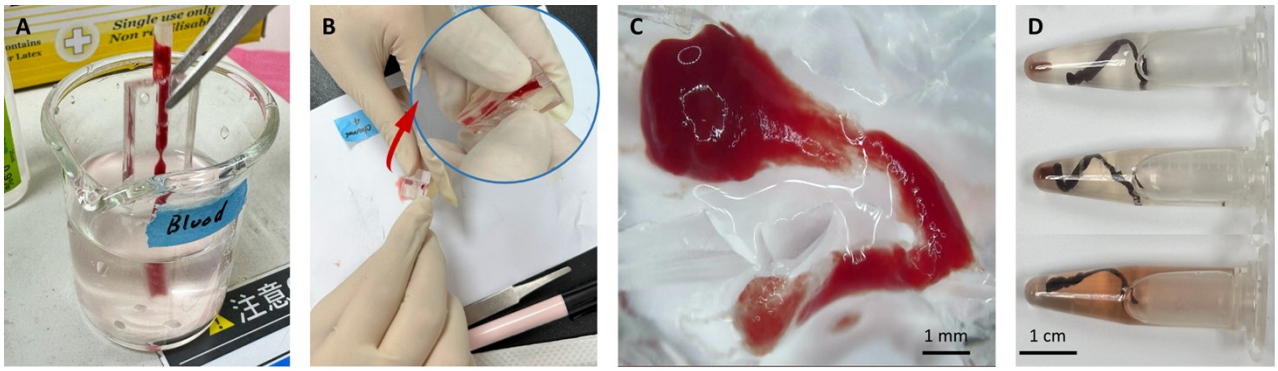

Supplementary Fig. S4 Clot analogue retrieval from the hourglass-profiled PDMS circular channel. A) The detached device was rinsed with PBS to remove residual blood. B) The PDMS slab was carefully opened from the side using a scalpel, and the formed clot analogue was gently retrieved with forceps. C) Representative image of a clot analogue formed under 1.8 mM $CaCl_2$, maintaining its elongated morphology and intact structure. D) Retrieved clot analogues formed under varying $CaCl_2$ concentrations (16.5, 12.6, and 6.6 mM, top to bottom).

Hematoxylin and eosin (H&E) staining

Formalin-fixed, paraffin-embedded tissue sections were deparaffinized and rehydrated through graded alcohols to distilled water. Sections were stained with Mayer's hematoxylin for 15 minutes, rinsed in running tap water for 5 minutes, and differentiated in 95% ethanol. Counterstaining was performed with eosin Y solution for 30 seconds to 1 minute. Slides were dehydrated through three changes of absolute ethanol, cleared in xylene (or substitute), and mounted with synthetic resin.

Martius scarlet blue (MSB) staining

Formalin-fixed, paraffin-embedded tissue sections were deparaffinized and rehydrated through graded alcohols to distilled water, then immersed in preheated Bouin's fluid (56–64 °C) for 60 minutes, followed by cooling for 10 minutes. After rinsing in tap water, sections were stained with freshly prepared Weigert's iron hematoxylin (2–5 minutes), rinsed, and sequentially stained with Martius yellow (2–3 minutes) and crystal scarlet (2–5 minutes). Differentiation was performed in phosphotungstic acid (2–10 minutes), followed by staining with aniline blue (2–5 minutes) until the desired intensity was achieved. Sections were dehydrated rapidly through absolute ethanol, cleared in xylene, and mounted with synthetic resin.

Oil Red O staining

Fresh or frozen tissue specimens were sectioned at 8–10 μm thickness and air-dried on glass slides. Sections were rinsed in tap water for 5–10 minutes, lightly counterstained with hematoxylin for 1–2 minutes, and washed again in tap water for 10 minutes. After rinsing with distilled water, sections were stained with freshly prepared Oil Red O working solution for 20–30 minutes, rinsed briefly to remove excess stain, and mounted using an aqueous medium or glycerin jelly.